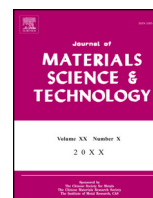




Contents lists available at ScienceDirect

Journal of Materials Science & Technology

journal homepage: www.jmst.org



Macro to nanoscale deformation of transformation-induced plasticity steels: Impact of aluminum on the microstructure and deformation behavior

V.S.Y. Injeti^a, Z.C. Li^a, B. Yu^a, R.D.K. Misra^{a,*}, Z.H. Cai^b, H. Ding^b

^a Department of Metallurgical, Materials and Biomedical Engineering, 500 W. University Avenue, USA

^b School of Materials Science and Engineering, Northeastern University, Shenyang 110819, China

ARTICLE INFO

Article history:

Received 14 August 2017

Received in revised form

27 September 2017

Accepted 1 November 2017

Available online xxx

Keywords:

Medium-manganese steels

Aluminum content

Electron microscopy

Mechanical properties

Nanoscale deformation

TRIP steel

Twinning

ABSTRACT

This work aims to elucidate the impact of aluminum-content on microstructure and deformation mechanisms of transformation-induced plasticity (TRIP) steels through macroscale and nanoscale deformation experiments combined with post-mortem electron microscopy of the deformed region. The solid-state transformation-induced mechanical deformation varied with the Al contents, and influenced tensile strength-ductility combination. Steels with 2–4 wt% Al were characterized by TRIP effect. In contrast to 2Al-TRIP and 4Al-TRIP steels, twinning-induced plasticity (TWIP) was also observed in conjunction with strain-induced martensite in 6Al-TRIP steel. This behavior is attributed to the increase in stacking fault energy with the increase of Al content and stability of austenite, which depends on the local chemical variation. The study addresses the knowledge gap with regard to the effect of Al content on austenite stability in medium-Mn TRIP steels. This combination is expected to potentially enable cost-effective alloy design with high strength-high ductility condition.

© 2017 Published by Elsevier Ltd on behalf of The editorial office of Journal of Materials Science & Technology.

1. Introduction

Conservation of energy and protection of environment are the primary factors that are considered important in the automotive industry. This requires reducing the weight of the automobiles in developing the next generation of high-strength steels. Transformation-induced plasticity (TRIP) steels are characterized by excellent combination of specific strength (strength/density) and are therefore suitable for automotive applications [1–3]. The TRIP effect depends on the content and degree of stability of retained austenite. Moreover, light-weight Al and Mg elements are added to TRIP steels to reduce the density [4,5].

Recent studies focused on Fe-(5–12)Mn-(0.1–0.2)C (wt%) TRIP steels [6–10]. For instance, Fe-5Mn-0.2C (wt%) steel exhibited good combination of tensile strength of 850–950 MPa and ductility of 20%–30% [10]. A high tensile strength of 1018 MPa and total elongation of 31% were obtained in Fe-7Mn-0.1C (wt%) steel [6]. Tensile strength of 1420 MPa with 31% total elongation was reported

for Fe-7Mn-0.2C (wt%) steel [7]. Fe-10Mn-0.14C-1.5Al (wt%) steel exhibited tensile strength of 1095 MPa and total elongation of 42% [11].

Aluminum is generally added to medium Mn (5%–12%) TRIP steels from the perspective of modulating austenite stability and reducing the probability of cementite formation [12]. Furthermore, Al in TRIP steels facilitates the presence of ferrite [13] and δ -ferrite during solidification and contributes to excellent tensile properties [14].

We have recently conducted a number of studies on the factors that governed structure-property relationship in hot-rolled and cold-rolled medium Mn TRIP steels containing Al [15–17]. In a previous study, the factors that governed the tensile properties were examined [15]. The aim here is to elucidate the impact of Al content on the mechanical stability of austenite and solid-state phase transformation of austenite to martensite. The aim was accomplished through a comparative analysis of macroscale tensile deformation and nanoscale deformation experiments. The underlying reasons for conducting nanoscale deformation experiments are listed in the experimental section. These experiments were combined with the post-mortem study of microstructural evolution of plastically deformed region by transmission electron microscopy. The obser-

* Corresponding author.

E-mail address: dmisra2@utep.edu (R.D.K. Misra).

Table 1
Chemical compositions of three experimental steels (wt%).

Steel	C	Mn	Al	Fe
Fe-11Mn-0.2C-2Al	0.22	11.2	1.95	86.63
Fe-11Mn-0.2C-4Al	0.18	11.02	3.81	84.99
Fe-11Mn-0.2C-6Al	0.21	10.75	6.08	82.96

ations on mechanical deformation are further corroborated in terms of stacking fault energy. We know that metastable retained austenite transforms to martensite when the chemical free energy required for solid-state transformation attains a critical threshold, which can be measured by stress-strain behavior [18–21]. This solid-state transformation induced by mechanical deformation impacts tensile strength-ductility combination because of strain-hardening effect [22,23]. Through macroscale and nanoscale deformation experiments in conjunction with electron microscopy, we expect to directly address the knowledge gap with regard to the effect of Al content (2%–6%, wt%) on the stability of austenite in medium-Mn TRIP steels. The outcome of the study is expected to potentially facilitate cost-effective alloy design of TRIP-steels with high strength-high ductility combination.

2. Experimental

The nominal chemical compositions of three experimental steels are listed in Table 1. 40 kg experimental steel ingots were cast in a vacuum induction furnace. The ingots were heated at 1200 °C for 2 h, hot forged into rods of section size 100 mm × 30 mm, then air cooled to room temperature (RT). Subsequently, the rods were soaked at 1200 °C for 2 h, hot-rolled to 4 mm thick strip in the temperature range of 1150–850 °C, and finally air cooled to room temperature (RT).

We have recently demonstrated that austenite reverted transformation (ART) heat treatment [9,24] (where the steel is cooled in water after austenitization, then intercritically heat treated for a long time and finally air cooled to room temperature) used for medium Mn steels is not applicable to the experimental steels studied here. The underlying reason is that the long intercritical heat treatment time renders austenite too stable and weakens the TRIP effect. Thus, quenching and tempering (Q&T) was envisioned by us as an alternative and effective heat treatment [25–27]. The as-hot-rolled sheets were subjected to Q&T heat treatment, as described previously [15]. The steels were heat treated at 650 °C for 1 h, followed by immediate quenching in water to room temperature. Next, they were tempered at 200 °C for 20 min and air cooled to ambient temperature. It was demonstrated [27] that the diffusion of carbon from ferrite to austenite during tempering, enhances the stability of austenite and thereby provides superior ductility through TRIP effect. Mn also diffuses during the heat treatment which significantly contributes to austenite stability, while Al promotes ferrite formation [13].

Tensile tests were carried out at room temperature using a universal testing machine (SANSCMT5000) at a constant crosshead speed of 3 mm min⁻¹. Tensile specimens of dimensions 12.5 mm width and 50 mm gage length were machined from the heat-treated sheets with tensile axis parallel to the rolling direction. The samples were etched with 25% sodium bisulfite solution. Microstructural examination was carried out using optical microscope (OM) and scanning electron microscope (SEM). The volume fraction of austenite was determined by X-ray diffraction (XRD) using CuK_α radiation. This involved the use of integrated intensities of (200)_α and (211)_α peaks and those of (200)_γ, (220)_γ and

(311)_γ peaks. The volume fraction of austenite V_A was calculated using the following equation [28]:

$$V_A = 1.4I_\gamma / (I_\alpha + 1.4I_\gamma) \quad (1)$$

where I_γ is the integrated intensity of austenite and I_α is the integrated intensity of α -phase.

Furthermore, the macroscale deformation during tensile experiments was studied by examining the tip of the fracture surface via TEM after making electron transparent foils from the tensile deformed region. We also conducted nanoscale deformation experiments using nanoindenter for the following reasons [29–34]. In nanoindentation, the indenter tip (20 nm radius in our case) is too small to produce a highly stressed volume beneath the indenter. The fundamental processes underlying discrete deformation in a small volume of the material is envisaged to have a low probability of encountering pre-existing dislocations prior to the commencement of plastic deformation. Furthermore, the tested volume is scalable with respect to the microstructure [29,30]. Moreover, the nanoindentation approach enables phase transformation and microstructural evolution to be studied through the analysis of nanoscale deformation data (load-displacement plots) combined with post-mortem electron microscopy of the plastically deformed region. The pop-ins in the load-displacement plots are generally indicative of phase transformation.

Given that the nanoindenters were subsequently examined by TEM for studying deformation mechanisms and associated microstructural evolution, the following procedure was adopted. First, 3 mm disks were punched from the experimental steels. To ensure that the nanoindenters were distributed along the thin area of the disk for examination via TEM, a modification of twin-jet electropolishing was developed. This was described in detail elsewhere [34]. In brief, the disks were partially jet electropolished in a refrigerated electrolyte containing 10% perchloric acid in acetic acid at 25 V for ~30 s to obtain a shining surface in the center part of the 3 mm disk, prior to nanoindentation experiments.

The partially polished disks, were subjected to nanoindentation experiments in displacement-controlled mode. The maximum displacement was set to 200 nm. The nanoindenter system Keysight G200XT consisted of a Berkovich three-sided pyramidal diamond indenter with a nominal angle of 65.3° and indenter tip radius of 20 nm. An array of indents of matrix 12 × 12 was defined with the indent gap of 10 μm. After the indentation experiments, the disks were removed from the mount and final electropolishing was carried out only from the side opposite to the indented surface. Using this procedure, the area surrounding the indents, which is present along the final jet-polished hole, was electron transparent to study the deformation behavior using a TEM (Hitachi H7600, 200 kV). A schematic illustration of the experimental procedure including sample preparation for nanoindentation experiments and subsequent examination of the plastic zone by TEM is presented in Scheme 1 (adapted from Ref. [34]).

Prior to the nanoindentation experiments, we ran a compliance calibration for the set-up and the tip was calibrated using fused silica provided with the instrument. The data presented in the manuscript were carefully analyzed and checked for excellent reproducibility of the “deformation data” and “indentation-induced deformation structures”.

3. Results and discussion

3.1. Microstructure

We first describe the microstructure prior to describing the deformation behavior. The microstructure of 2Al-TRIP, 4Al-TRIP and 6Al-TRIP steels is presented in Fig. 1(a)–(c), respectively. In the

Download English Version:

<https://daneshyari.com/en/article/7951985>

Download Persian Version:

<https://daneshyari.com/article/7951985>

[Daneshyari.com](https://daneshyari.com)